

# The Impact of Social Attractiveness on Casual Group Formation: Power-Law Group Sizes and Suppressed Percolation

Matheus S. Mariano<sup>1</sup> and José F. Fontanari<sup>1</sup>

<sup>1</sup>Instituto de Física de São Carlos, Universidade de São Paulo, São Carlos, 13560-970, São Paulo, Brazil.

## Abstract

The dynamics of casual group formation has long been a subject of interest in social sciences. While early stochastic models offered foundational insights into group size distributions, they often simplified individual behaviors and lacked mechanisms for heterogeneous social appeal. Here, we re-examine the attractiveness-driven interaction model, an agent-based framework where point-like agents move randomly in a 2D arena and exhibit varied social appeal, leading them to pause near highly attractive celebrity peers. We compare this model to a null model where the agents are continuously in movement, which resembles a Random Geometric Graph. Our extensive simulations reveal significant structural and dynamic differences: unlike the null model, the attractiveness-driven model's average degree increases linearly with system size for fixed density, resulting in more compact groups and the suppression of a percolation transition. Crucially, while the null model's group size distribution is either exponentially decaying or bimodal, the attractiveness-driven model robustly exhibits a power-law distribution,  $P(n) \propto n^{-2.5}$ , with an exponent independent of density. These findings, obtained through computationally intensive simulations due to long equilibration times, offer a thorough quantitative characterization of this model, highlighting the critical role of individual attractiveness in shaping social aggregation in physical space.

**Keywords:** face-to-face interactions, casual groups, power-law distribution

# 1 Introduction

Human social life in public settings is fundamentally characterized by the dynamic formation and dissolution of temporary, face-to-face interactions, which spontaneously give rise to casual groups [1, 2]. The intricate ebb and flow of individuals forming and leaving these free-forming clusters – whether observed in a bustling cocktail party or the steady stream of pedestrians on a sidewalk – has long captivated researchers across social sciences [3, 4]. Pioneering stochastic models from the 1960s laid crucial groundwork for understanding the size distributions of such groups, often by simplifying individual behaviors and abstracting away specific personal attributes [5]. However, the recent advent of large-scale empirical data [6] and sophisticated agent-based modeling techniques has opened unprecedented avenues for a more nuanced and quantitative understanding of these complex social systems. Our work bridges these classical sociological insights with contemporary computational approaches by characterizing the statistical properties of casual groups within a model that explicitly incorporates heterogeneous social appeal among agents [7, 8], a critical factor largely absent from earlier theoretical constructs [3–5].

Specifically, we re-examine an agent-based model for face-to-face interactions developed by Starnini et al. [7, 8], which posits point-like agents moving randomly within a two-dimensional square arena. A key feature of this model is the heterogeneous attractiveness assigned to agents, where some exhibit particularly high appeal, who we refer to as celebrities. Agents are more likely to pause their random movement and thus prolong interaction when they are within the interaction zone of these attractive peers. It is due to this core interaction mechanism that we refer to the model as the attractiveness-driven interaction model. While the original studies primarily focused on the temporal properties of face-to-face interactions, such as contact durations and inter-event times, our research shifts the emphasis to the equilibrium properties of the emergent spatial contact network, where groups are naturally defined as connected components within this graph [9].

To fully appreciate the impact of celebrity presence, we compare the attractiveness-driven interaction model against a null model. In this null model, agents are continuously in motion, rendering agents’ attractiveness, whether heterogeneous or not, irrelevant to interaction durations. This null model shares similarities with the classic Random Geometric Graph (RGG) [10, 11]. Our findings reveal a stark contrast: while the average degree of the null model depends solely on density, the average degree in the attractiveness-driven interaction model increases linearly with the arena’s linear size for a fixed density. This implies that as the system scales up, the clusters forming around celebrity agents become increasingly compact. Crucially, this enhanced clustering around celebrities actively prevents the formation of a single, large cluster encompassing most agents, thereby eliminating the percolation transition that characterizes the fraction of agents in the largest group in both the null model and the RGG [12].

Beyond these network-level properties, a particularly important result concerns the distribution of group sizes  $P(n)$ , which is widely considered the preferred empirical measure for characterizing casual groups [3–5]. Our analysis reveals a distinct behavior across the models: while the null model yields a group size distribution that decays

exponentially with increasing group size  $n$  for low densities, transitioning to a bimodal distribution at higher densities [12], the attractiveness-driven interaction model surprisingly produces a power-law distribution,  $P(n) \propto n^{-\beta}$  with  $\beta = 2.5$ . Notably, the power-law exponent  $\beta$  appears to be independent of density, highlighting a robust emergent property driven by heterogeneous social appeal.

While our study focuses on casual groups, it is useful to distinguish them from the more stable concept of communities prevalent in complex network analysis. Within the framework of complex networks, a community is typically defined as a densely interconnected group of nodes that has sparser connections to the rest of the network [9]. These communities are ubiquitous in social and biological systems and are often understood to represent relatively enduring social groupings, driven by shared interests, background, or persistent relationships [13]. However, a crucial distinction from casual groups lies in their temporal stability: complex network communities are generally characterized by their relative persistence over time. This inherent stability makes them fundamentally different from the transient, fleeting nature of casual groups, which are continuously forming and dissolving. Consequently, despite their utility in characterizing more permanent social structures, such communities are not ideal models for the rapidly evolving dynamics of casual groups, which are better captured by models of face-to-face interaction networks.

The remainder of this paper is organized as follows. In section 2, we provide a detailed description of the asynchronous agent-based model dynamics, including the rules governing agent movement and interaction. Section 3 presents our comprehensive simulation findings. Particular attention is drawn to the exceptionally large timescales required for the attractiveness-driven interaction model to reach equilibrium—a state where macroscopic quantities such as the average degree and the fraction of agents in the largest group stabilize around time-independent values. Consequently, studying the attractiveness-driven interaction model proves to be highly computationally intensive, even for relatively small arena sizes. Finally, section 4 summarizes our main findings and presents future work directions.

## 2 The model

Following Starnini et al. [7, 8], we investigate the properties of groups emerging from face-to-face interactions within a system of  $N$  point-like agents. These agents move in a square arena of linear size  $L$ , with periodic boundary conditions, resulting in a density  $\rho = N/L^2$ . Interactions occur between agents within a distance  $d$ , and agents perform a random walk, moving a fixed step of length  $v$  in a randomly chosen direction. Consistent with the original model, we set  $v = d = 1$ .

A crucial feature of this model is that each agent  $i \in \{1, \dots, N\}$  possesses an intrinsic attractiveness or social appeal  $a_i \in [0, 1]$ . This value quantifies an agent’s ability to capture the interest of others, specifically by influencing their willingness to cease movement and maintain an interaction. The model also distinguishes between two classes of agents: active and inactive. Inactive agents become active with a probability  $r_i \in [0, 1]$ . Only active agents can interact and move; they transition to an inactive state with probability  $1 - r_i$  when isolated. Both the attractiveness  $a_i$  and the

activation probability  $r_i$  are assigned randomly from the unit interval at time  $t = 0$  for each agent and remain fixed throughout the simulation.

The dynamics of this asynchronous face-to-face interaction model begins with agents randomly distributed in the arena at  $t = 0$  and proceed as follows. At each time step  $\delta t = 1/N$ , a focal agent, say agent  $i$ , is randomly selected.

- If agent  $i$  is inactive: it attempts to become active with probability  $r_i$ . If this attempt fails, it remains inactive.
- If agent  $i$  is active:
  - Decision to move: agent  $i$  assesses the attractiveness of all other active agents within its interaction distance  $d$ . It then decides to move with a probability  $p_i(t)$  defined as

$$p_i(t) = 1 - \max_{j \in \mathcal{N}_i(t)} \{a_j\}, \quad (1)$$

where  $\mathcal{N}_i(t)$  represents the set of active neighbors of agent  $i$  at time  $t$ . Notably, an active agent with no active neighbors (i.e.,  $\mathcal{N}_i(t) = \emptyset$ ) will always choose to move.

- Movement: if agent  $i$  decides to move, it selects a random direction within  $[0, 2\pi)$  and moves a step of length  $v$ .
- Inactivation: after moving, if agent  $i$  finds itself isolated (i.e., no other active agents are in its neighborhood), it may become inactive with probability  $1 - r_i$ .

The asynchronous update scheme, characterized by a time increment  $\delta t = 1/N$ , ensures that exactly  $N$  agents are selected as focal agents during the interval from  $t$  to  $t + 1$ , though some agents may be selected multiple times.

The structure of the groups formed by these face-to-face interactions is illuminated by creating an edge between any two active agents within distance  $d$ , thereby forming an undirected contact graph. A group is defined as a connected component within this graph [9], meaning it is a subgraph where every active agent can reach every other active agent within that subgraph. Inactive agents do not interact, are invisible to other agents, and thus do not belong to any group. They can be conceptualized as agents momentarily outside the interaction arena.

The most distinctive and powerful feature of the agent-based model proposed by Starnini et al. [7, 8], which we term the attractiveness-driven interaction model, lies in its incorporation of heterogeneous social appeal among agents. This heterogeneity allows us to conceptually frame agents with significant social appeal as celebrities, providing a natural and elegant generalization of the casual group models developed in the 1960s [3, 5] (for a more recent contribution on casual groups, see [14, 15]). Unlike those earlier models, which typically described temporary groups formed in settings not dominated by a few highly influential individuals [5], the attractiveness-driven interaction model explicitly accounts for such celebrity effects.

### 3 Results

To thoroughly understand the impact of celebrity presence on temporary group statistics, our findings are compared against a null model. In this null model, we set  $a_i = 0$  for all agents, meaning active agents never cease movement. This setup bears strong

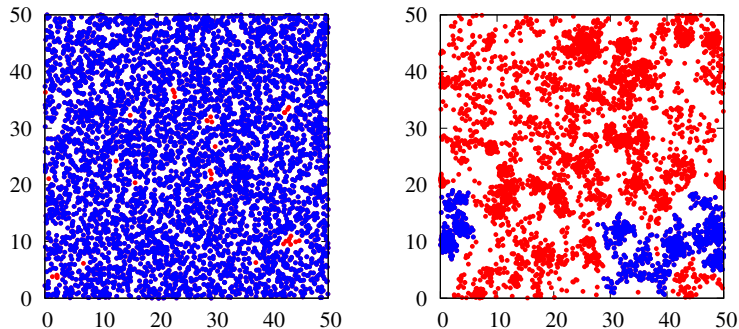


**Fig. 1** Spatial distribution of active agents at  $t = 10^5$ . Snapshots illustrate the spatial distribution of active agents (red symbols) for the null model (left panel) and the attractiveness-driven interaction model (right panel). Active agents belonging to the largest group are highlighted in blue. In the null model, the largest cluster contains 4890 agents, compared to 1226 agents in the attractiveness-driven interaction model. Simulation parameters are  $L = 50$  and  $N = 5000$ .

resemblances to, though is not identical to, the classic Random Geometric Graph (RGG). Introduced in the 1960s to model wireless communication networks [10, 11], the RGG’s properties, particularly its threshold phenomena, have been extensively explored in statistical physics [12]. Furthermore, the RGG has become a preferred framework for modeling various phenomena, including synchronization [16], opinion dynamics [17, 18], epidemic spreading [19], and cooperative problem-solving [20] in scenarios where agents move randomly within geographically constrained regions. A key characteristic of the RGG is its spatially homogeneous distribution of agents, uniformly and randomly placed within the square arena, which facilitates the derivation of analytical results [11]. The primary distinction between our null model and the RGG lies in the treatment of isolated agents: the RGG typically features more isolated agents, since in our null model, isolated agents can become inactive and effectively be removed from the contact graph. Nevertheless, at sufficiently high densities where isolated agents are rare, both models yield identical results.

Figure 1 presents snapshots of the spatial distribution of active agents at  $t = 10^5$  for the null model and the attractiveness-driven interaction model, at a density  $\rho = 2$ . At this density, the null model typically shows nearly all agents belonging to a single large group. In stark contrast, the attractiveness-driven interaction model reveals agents dispersed into several groups of comparable sizes. To quantitatively assess this inhomogeneity in spatial distribution, we calculate the pair correlation function  $g(r)$ , which represents the fraction of pairs of active agents whose distance falls between  $r$  and  $r + \delta r$ . Due to periodic boundary conditions, the maximum possible distance between any two agents is  $L/\sqrt{2}$ . Importantly,  $g(r)$  is independent of  $N$ . In fact,

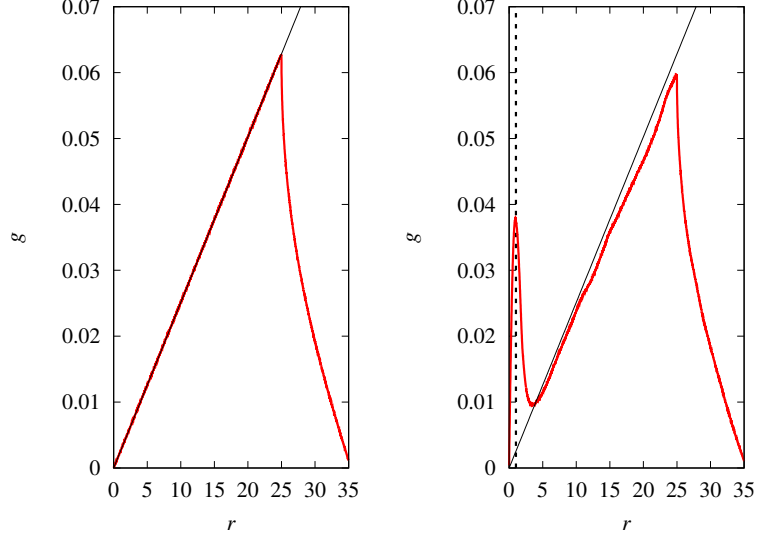


**Fig. 2** Pair correlation function  $g(r)$  at  $t = 10^5$ . The pair correlation function is shown for the null model (left panel) and the attractiveness-driven interaction model (right panel). Results are averaged over 100 independent simulation runs. The thin black line represents the analytical result for uniformly randomly distributed agents,  $g(r) = 2\pi r/L^2$ , which is valid for  $r < L/2$ . The vertical dashed line indicates  $r = d = 1$ . Simulation parameters are  $L = 50$  and  $N = 5000$ .

$N$  solely determines the number of samples,  $N(N - 1)/2$ , used to estimate  $g(r)$  in each simulation run. For uniformly randomly distributed agents,  $g(r) = 2\pi r/L^2$  for  $r < L/2$ , a range where boundary conditions do not affect distance calculations. Figure 2 displays the pair correlation function computed using  $\delta r = 0.01$ . The results for the null model closely align with the pair correlation function of uniformly randomly distributed agents for  $r < L/2$ . Conversely, the attractiveness-driven interaction model exhibits a pronounced peak at  $r = d = 1$  in its pair correlation function, quantitatively confirming the significantly higher occurrence of closely clustered agents, as qualitatively observed in Fig. 1.

A significant aspect of studying the attractiveness-driven interaction model is the time required for the dynamics to reach a stationary regime. In this regime, macroscopic parameters, such as the graph's average degree  $k$ , exhibit only small fluctuations around a stable, time-independent value. Figure 3 illustrates the time dependence of  $k$  at a fixed density of  $\rho = 0.6$ . The left panel, presenting results for the null model, shows that the system quickly attains a stationary state, which is largely independent of the arena's linear size  $L$  as long as  $L$  is not too small. These results highlight a key difference between our null model and the RGG. In the RGG, the  $N$  agents are assumed to be homogeneously distributed in the arena, leading to an average degree equal to the mean number of agents within a unit radius circle centered on a focal agent, i.e.,  $k = \pi\rho$ . Considering that in both our null and attractiveness-driven interaction models agents are initially randomly distributed at  $t = 0$ , but, on average, only half are active, our initial prediction would be  $k = \pi\rho/2$ . This prediction perfectly aligns with our simulation results at  $t = 0$ . However, as the agents move randomly within the

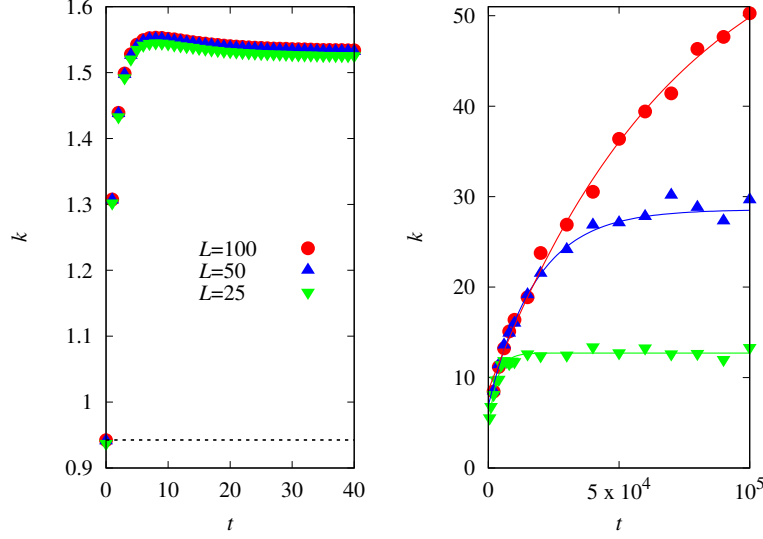


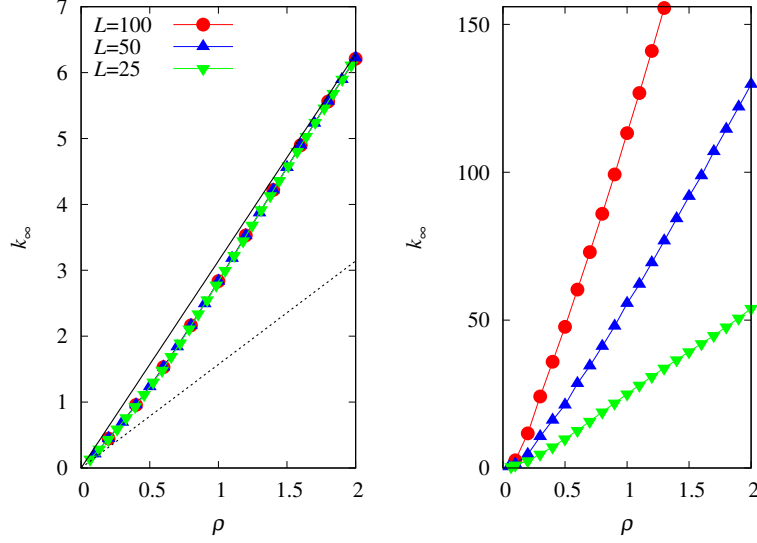
**Fig. 3** Time evolution of average degree. Average degree  $k$  as a function of time  $t$  for the null model (left panel) and the attractiveness-driven interaction model (right panel). Results are shown for  $\rho = 0.6$  and varying linear sizes  $L = 25, 50$ , and  $100$ . Data points (symbols) represent averages obtained from  $10^3$  independent simulation runs. In the left panel, the horizontal dashed line indicates the analytical prediction  $k = \pi\rho/2$ . In the right panel, the solid colored curves correspond to the exponential fit function given by eq. (2).

arena, the mean degree of the null model becomes considerably greater than this initial prediction from the homogeneous distribution assumption. This deviation occurs because only isolated agents can become inactive, and since our undirected graphs are formed exclusively by active agents, there are effectively fewer isolated agents in our null model compared to a pure RGG, consequently leading to a higher average degree.

In contrast to the null model, the attractiveness-driven interaction model necessitates considerably longer timescales to achieve equilibrium. Both the equilibrium values and the time required to reach this state exhibit a strong dependence on  $L$ , as depicted in the right panel of Fig. 3. These quantities can be estimated by fitting the time evolution of the average degree  $k(t)$  to the exponential function

$$k(t) = k_{\infty} - k^* \exp(-t/\tau_k) \quad (2)$$

in the region  $t \in [500, 2 \times 10^5]$ . Here,  $k_{\infty}$ ,  $k^*$ , and  $\tau_k$  are the fit parameters that vary with the density  $\rho$  and the linear size  $L$ . We observe that the characteristic relaxation time  $\tau_k$  increases proportionally with  $L^2$  (or with  $N$ , given a fixed density). This significant dependence severely constrains the maximum system size that can be feasibly studied through simulations. This behavior reflects the inherent difficulty in breaking down an initially homogeneous configuration of agents into distinct clusters centered around a few celebrities, as well as the ongoing competition among these influential agents for followers.



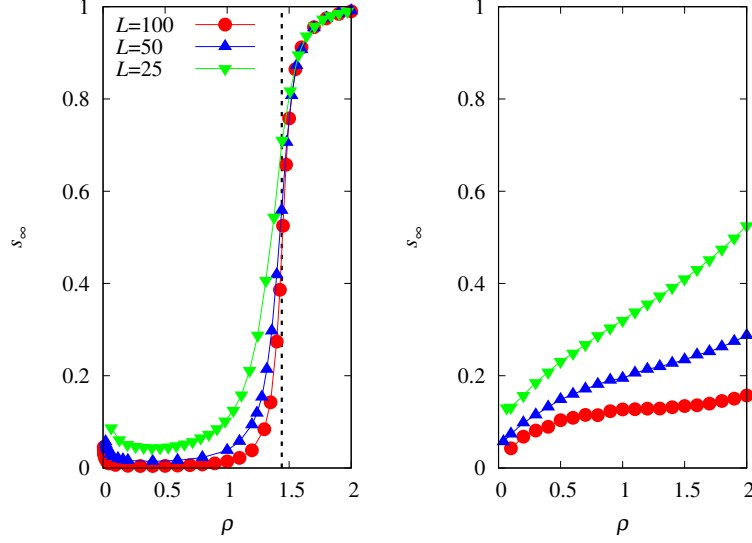
**Fig. 4** Equilibrium average degree as a function of density. Equilibrium average degree  $k_\infty$  for the null model (left panel) and the attractiveness-driven interaction model (right panel) as functions of density  $\rho$ . Results are shown for linear sizes  $L = 25, 50$ , and  $100$ . Data points (symbols) represent averages obtained from  $10^3$  independent simulation runs. In the left panel, the solid black line denotes  $k = \pi\rho$ , while the dashed black line indicates  $k = \pi\rho/2$ . Lines connecting the symbols serve as visual guides.

Figure 4 illustrates the dependence of the equilibrium average degree  $k_\infty$  on the density  $\rho$ . The left panel demonstrates that for the null model  $k_\infty$  depends solely on density, consistent with the observations in Fig. 3. However, its specific dependence on  $\rho$  diverges from that of a pure RGG. Specifically, for an RGG, the average degree is  $k = \pi\rho$  if all agents are active, and  $k = \pi\rho/2$  if, on average, only half of the agents are active. Our null model aligns with RGG predictions at density extremes: at high densities, where isolated agents are rare, most agents remain active, leading to results consistent with  $k = \pi\rho$ . Conversely, at low densities, where many agents are isolated and thus often inactive, results align with  $k = \pi\rho/2$ .

The right panel of Fig. 4 presents the results for the attractiveness-driven interaction model. For a fixed  $L$ , increasing  $\rho$  is equivalent to increasing  $N$ , so a linear increase in  $k_\infty$  with respect to  $\rho$  is generally expected, provided the density is not too low. As noted previously, at very small densities, an increase in  $N$  does not directly translate into a proportional increase in the number of active nodes in the graph due to the potential for isolated agents to become inactive. The remarkable finding, however, is the increase in  $k_\infty$  with increasing  $L$  when the density  $\rho$  is held constant. This indicates that as the number of agents  $N$  and the linear size  $L$  increase simultaneously while maintaining a constant density, the groups forming around celebrities become increasingly compact.

Another quantity of significant interest, particularly from the perspective of statistical physics [21], is the fraction of active agents belonging to the largest group. We denote this fraction by  $s$ , which ranges from  $1/N_{act}$  (indicating all groups are isolates)





**Fig. 5** Equilibrium fraction of active agents in the largest group. Equilibrium fraction of active agents in the largest group  $s_\infty$  for the null model (left panel) and the attractiveness-driven interaction model (right panel) as function of density  $\rho$ . Results are shown for linear sizes  $L = 25, 50$ , and  $100$ . Data points (symbols) represent averages obtained from  $10^3$  independent simulation runs. In the left panel, the vertical dashed line indicates the critical density  $\rho_c \approx 1.44$  of the Random Geometric Graph (RGG). Lines connecting the symbols serve as visual guides.

to 1 (implying all active agents belong to a single group). Here,  $N_{act}$  represents the total number of active agents, a value dependent on both  $\rho$  and  $L$ . The snapshots presented in Fig. 1 qualitatively illustrate the striking difference in the largest group size between the null and attractiveness-driven interaction model at high density. To quantitatively estimate the equilibrium value of  $s$ , denoted as  $s_\infty$ , we employ a procedure analogous to that used for  $k_\infty$ . Specifically, we measure  $s$  at various times and fit the resulting data to the exponential function

$$s(t) = s_\infty - s^* \exp(-t/\tau_s) \quad (3)$$

for values of  $t$  in the region  $t \in [500, 2 \times 10^5]$ . As with the previous fit,  $s_\infty$ ,  $s^*$ , and  $\tau_s$  are the extracted fit parameters.

The left panel of Fig. 5 presents the results for the null model. In this model,  $s_\infty$  exhibits a discontinuity at a critical density  $\rho_c$  in the thermodynamic limit. Specifically, as  $L \rightarrow \infty$ ,  $s_\infty \rightarrow 0$  for  $\rho < \rho_c$ , and  $s_\infty$  becomes positive otherwise. For high densities, where the null model is effectively identical to the RGG, the figure shows an estimated  $\rho_c \approx 1.44$  for the RGG [12]. Interestingly, at very low densities,  $s_\infty$  is observed to increase as  $\rho$  decreases for a fixed  $L$ . This counter-intuitive behavior occurs because the number of active agents,  $N_{act}$  (which forms the denominator in the definition of  $s$ ), decreases significantly at low densities due to a higher proportion of agents becoming inactive. Thus, it is not that the number of active agents within the largest group

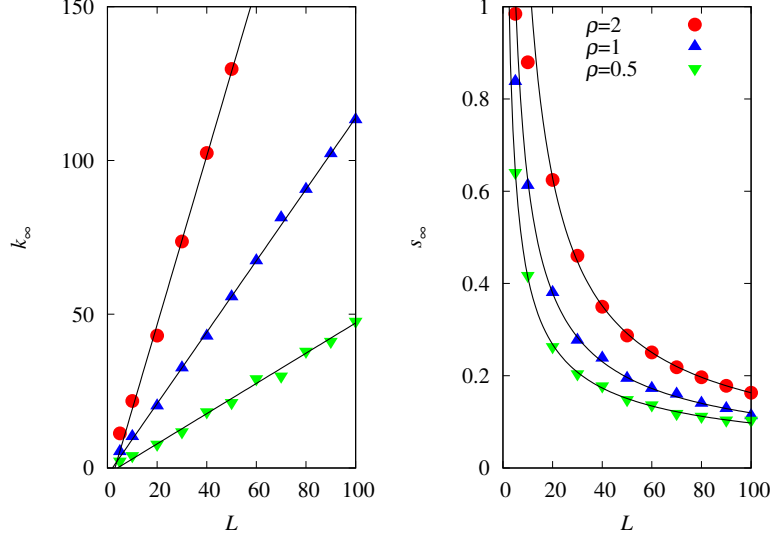


**Fig. 6** Equilibrium average degree and largest group fraction vs. linear system size. Equilibrium average degree  $k_\infty$  (left panel) and fraction of active agents in the largest group  $s_\infty$  (right panel) for the attractiveness-driven interaction model as functions of the linear size  $L$  of the square arena. Results are shown for densities  $\rho = 0.5, 1$  and  $2$ . Data points (symbols) represent averages obtained from  $10^3$  independent simulation runs. In the left panel, the straight lines depict the linear fit  $k_\infty = aL + b$ . In the right panel, the curves illustrate the power-law fit  $s_\infty = aL^{-b}$ , where  $a$  and  $b$  are fit parameters for both cases. The fitting region for all curves is  $L > 20$ .

increases. Rather, the total pool of active agents shrinks, leading to a larger fraction of these agents belonging to the dominant group.

In contrast, the results for the attractiveness-driven interaction model, shown in the right panel of Fig. 5, do not exhibit a threshold phenomenon. However, they strongly support the scenario of highly compact clusters of followers forming around a few celebrities. The slow and smooth increase in  $s_\infty$  with  $\rho$  indicates that active agents are distributed relatively uniformly among these compact groups without significantly increasing their spatial extension. Such an uncontrolled spatial increase would eventually lead to a sharp percolation transition similar to those observed in the null model and the RGG. While groups will eventually begin to merge at sufficiently high densities, causing  $s_\infty$  to approach 1, this process is notably slow and smooth, distinctly lacking the threshold behavior of the null model.

Figure 6 summarizes the dependence of the equilibrium quantities  $k_\infty$  and  $s_\infty$  on the linear size  $L$  of the square arena for the attractiveness-driven interaction model. As shown in the left panel, the average degree  $k_\infty$  increases linearly with  $L$  (or proportionally to  $N^{1/2}$  when density  $\rho$  is fixed). This implies that, on average, the number of active agents within an interaction distance  $d = 1$  from an active agent scales with  $N^{1/2}$ . The right panel reveals that  $s_\infty$  decays as a power law, specifically as  $1/L^\gamma$ , when  $L$  increases. The exponent  $\gamma$  ranges from approximately 0.6 for  $\rho = 0.5$  to 0.8 for  $\rho = 2$ . Precisely determining this power-law decay and accurately estimating the exponent  $\gamma$  would, of course, necessitate simulations with significantly larger values of

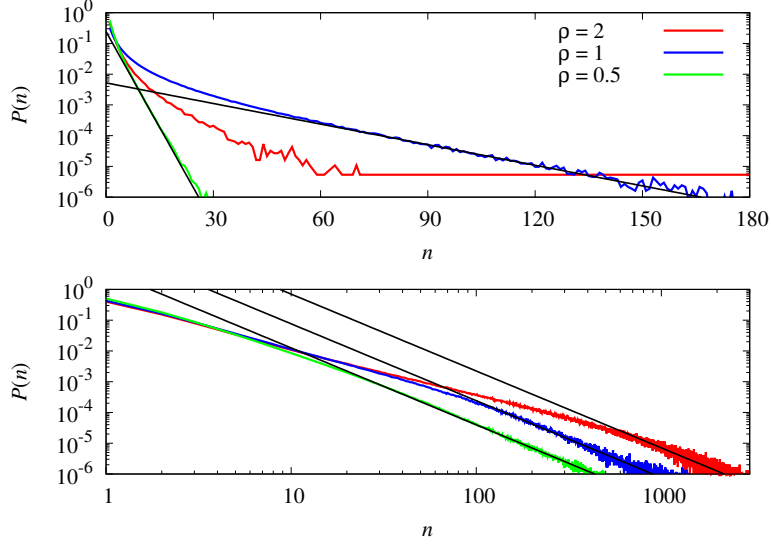


**Fig. 7** Group size distribution at  $t = 10^5$ . Distribution of group sizes  $P(n)$  for the null model (top panel) and the attractiveness-driven interaction model (bottom panel) with linear size  $L = 50$ . Results are shown for densities  $\rho = 0.5, 1$ , and  $2$ . These distributions were estimated using  $10^4$  to  $10^5$  independent simulation runs. In the top panel, the black lines represent exponential fits to the data for  $\rho = 0.5$  and  $1$ . In the bottom panel, the black lines depict power-law fits  $P(n) \propto n^{-\beta}$  with  $\beta = 2.5$ .

$L$  than those considered here. Assuming that the number of active agents  $N_{act}$  grows linearly with  $N$ , the absolute number of agents in the largest group (i.e.,  $s_{\infty} N_{act}$ ) scales approximately with  $N^{1-\gamma/2}$ .

In the study of casual groups, a primary quantity of interest is the mean fraction of groups of a given size  $n$ , with  $n = 1, \dots, N$ , at equilibrium [3, 5, 14]. This fraction can be interpreted as the probability of observing a group of size  $n$ , denoted as  $P(n)$ . Empirical studies typically aggregate observations of groups of the same size across numerous occasions – for instance, counting pedestrian groups on a sidewalk over many spring mornings [3]. They then report the ratio of the total count of groups of a specific size to the total number of groups observed. In our computational context, this approach is equivalent to combining groups identified from multiple independent simulation runs. Figure 7 summarizes our findings for  $P(n)$  across three distinct density values.

For the null model,  $P(n)$  exhibits an exponential decay for large  $n$ , provided that  $\rho < \rho_c$ . For densities exceeding  $\rho_c$ , the distribution of group sizes becomes bimodal, though the secondary peak is not visible at the scale of Fig. 7 (top panel). It features a prominent, high peak at  $n = 1$  (isolated agents) and a smoother, secondary peak for  $n$  values close to  $N$ . This behavior is consistent with findings for the RGG [12] and reflects the emergence of a large group that encompasses most of the active agents in each simulation run. The average size of this largest group is shown in Fig. 5.

Characterizing the group size distribution for the attractiveness-driven interaction model, shown in the bottom panel of Fig. 7, proves to be quite challenging. While a

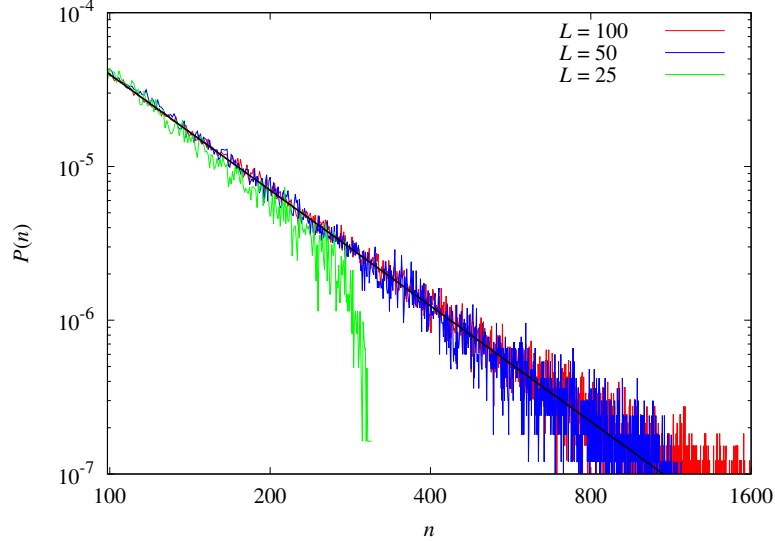


**Fig. 8** Group size distribution dependence on system size at  $t = 10^5$ . Distribution of group sizes  $P(n)$  for the attractiveness-driven interaction model at  $\rho = 0.5$ . Results are shown for linear sizes  $L = 25, 50$ , and  $100$ . These distributions were estimated using  $10^5$  independent simulation runs. The black line represents the power-law fit  $P(n) \propto n^{-\beta}$  with  $\beta = 2.5$ .

power-law decay was initially suggested in a previous study of the model, the relatively small number of agents considered in that work ( $N = 400$ ) does not permit such an inference [8]. Furthermore, direct fitting of the asymptotic behavior of  $P(n)$  using a variety of fit distributions [22] proved inconclusive, primarily due to a strong dependence on the chosen fit range. However, a valuable insight about the fit range is gained by examining the dependence of  $P(n)$  on the number of agents  $N$  (or the linear size  $L$  of the system) at a fixed density, as presented in Fig. 8. The value  $\rho = 0.5$  was selected as it allows us to obtain extensive statistics across the three system sizes considered.

The group size distribution for  $L = 25$  ( $N = 312$ ) clearly exhibits a sharp cutoff around  $n = 312$ , which corresponds to the maximum possible group size for that arena. By extension, we infer that the cutoffs for  $L = 50$  and  $L = 100$  should occur around  $n = 1250$  and  $n = 5000$ , respectively. Our approach for defining the asymptotic fit region is to select the range just before the onset of this cutoff for a given system size. As depicted in Fig. 8, a power-law  $P(n) \propto n^{-\beta}$  with  $\beta = 2.5$  provides an excellent fit to the data. However, a significant challenge arises from the fact that this asymptotic regime sets in for  $n > 100$ , where  $P(n)$  is already very small. Consequently, producing reliable statistics necessitates an extremely large number of samples. For instance, the distribution for  $L = 100$  required approximately  $10^8$  groups for its estimation. This makes demonstrating the power-law fit over two or more orders of magnitude practically unfeasible. The situation further exacerbates with increasing density, as the asymptotic regime shifts to even larger  $n$ . Nevertheless, having now identified a reliable fit region, we find that the same power-law also describes the data accurately for high densities (see bottom panel of Fig. 7). This consistency is not surprising,

given our earlier analysis (see Fig. 5) demonstrating that the attractiveness-driven interaction model’s properties are not critically dependent on density.

## 4 Conclusion

The attractiveness-driven interaction model introduced by Starnini et al. [7, 8] has significantly advanced our understanding of human contact dynamics, particularly in describing the temporal dimension of face-to-face interactions. While their original studies primarily focused on distributions of contact times and inter-event times, our research extends this framework by characterizing the sizes of casual, or temporary, groups formed by agents within their contact zones. Aligning with the foundational studies of casual groups from the 1960s [3, 5], our analysis centers on the equilibrium regime, where macroscopic quantities like average degree and the fraction of agents in the largest group stabilize over time (see Fig. 3).

In addition to introducing a spatial dimension to the casual group formation dynamics, which requires defining groups as connected components of the contact graph, the attractiveness-driven interaction model uniquely incorporates the notion of an agent’s attractiveness or social appeal  $a_i$  for  $i = 1, \dots, N$ . This appeal is associated with the probability that other agents will pause their movement when in contact with agent  $i$  [7]. We followed the original model by considering  $a_i$  to be uniformly distributed within the unit interval. Agents with high social appeal, specifically those with  $a_i \approx 1$ , can be conceptually considered celebrities. This represents a realistic feature to be included in models of casual human groups, a characteristic that previous foundational studies [5] explicitly omitted. We found that the presence of these celebrities profoundly impacts the statistical properties of casual groups, yielding striking differences when compared to the null (agent-homogeneous) model, where  $a_i = 0$  for all agents, implying continuous movement for all active participants.

The most significant distinction between the attractiveness-driven interaction model and the null model lies in the average degree  $k$  of the contact graph (see Fig. 4). In the null model, as in the Random Geometric Graph (RGG),  $k$  is solely a function of density. In sharp contrast, for the attractiveness-driven interaction model,  $k$  increases linearly with the arena’s linear size  $L$  (or with  $N^{1/2}$ ) for fixed density. This implies that as both  $L$  and  $N$  increase simultaneously to maintain constant density, the number of agents within the interaction zone (i.e., within a distance of  $d = 1$ ) of a given agent remains constant in the null model, but increases linearly with  $L$  in the attractiveness-driven interaction model. Consequently, groups become more compact as  $L$  increases. This clustering of agents into compact groups around celebrities prevents the abrupt formation of a single large group encompassing most agents in the arena. In fact, the equilibrium fraction of agents in the largest group ( $s_\infty$ ) increases smoothly with density, notably lacking the percolation transition observed in the null model and the RGG (see Fig. 5).

The distribution of group sizes  $P(n)$  is arguably the simplest quantitative information obtainable from direct observation of casual groups. For small gatherings ( $N = 20$ ) without celebrity effects, empirical results are often well described by a zero-truncated Poisson distribution [3]. The situation becomes more complex for larger gatherings

( $N = 400$ ), where empirical distributions have been suggested to be compatible with power-law behavior [8]. Our extended analysis of the attractiveness-driven interaction model using system sizes up to  $N = 5000$  indicates that  $P(n)$  is well described by a power law in its asymptotic regime, specifically  $P(n) \propto n^{-\beta}$ . Although computationally very challenging to reach and reliably characterize this regime, the power-law exponent appears to be independent of density, with a value of  $\beta = 2.5$  (see Figs. 7 and 8).

This study highlights the critical role of individual social appeal in shaping the macro-scale structure and dynamics of human contact networks, effectively bridging contemporary agent-based modeling [7, 8] with classical sociological insights into casual group formation [3, 5]. By demonstrating how the heterogeneous distribution of attractiveness, or the presence of celebrities, fundamentally alters group cohesion, connectivity, and emergent properties like percolation, our re-examination of the attractiveness-driven interaction model offers a thorough quantitative characterization. Future work will explore the implications of attractiveness distributions that more closely mirror real-world social hierarchies, such as wealth distribution [23], and consider the inclusion of a repulsive hard core for agents, mimicking the comfort distance observed in humans [24] and animals [25], thereby further enriching the predictive power of these models for social aggregation in physical space.

**Acknowledgments.** JFF is partially supported by Conselho Nacional de Desenvolvimento Científico e Tecnológico grant number 305620/2021-5. MSM is supported by Fundação de Amparo à Pesquisa do Estado de São Paulo (FAPESP) grant number 2024/00582-4. This research is partially supported by Fundação de Amparo à Ciência e Tecnologia do Estado de Pernambuco (FACEPE) grant number APQ-1129-1.05/24.

## References

- [1] Coleman J S 1964 *Introduction to Mathematical Sociology* (London: Free Press Glencoe)
- [2] Burgess J W 1984 Do Humans Show a “Species-Typical” Group Size?: Age, sex, and environmental differences in the size and composition of naturally-occurring casual groups *Ethol. Sociobiol.* **5** 51–57
- [3] Coleman J S and James J 1961 The Equilibrium Size Distribution of Freely-forming Groups *Sociometry* **24** 36–45
- [4] Cohen J E 1971 *Casual Groups of Monkeys and Men* (Cambridge: Harvard University Press)
- [5] White H 1962 Chance Models of Systems of Casual Groups *Sociometry* **25** 153–172
- [6] Cattuto C, Van den Broeck W, Barrat A, Colizza V, Pinton J-F and Vespignani A 2010 Dynamics of person-to-person interactions from distributed RFID sensor networks *PLoS ONE* **5** e11596

- [7] Starnini M, Baronchelli A and Pastor-Satorras R 2013 Modeling Human Dynamics of Face-to-Face Interaction Networks *Phys. Rev. Lett.* **110** 168701
- [8] Starnini M, Baronchelli A and Pastor-Satorras R 2016 Model reproduces individual, group and collective dynamics of human contact networks. *Soc. Netw.* **47** 130–137
- [9] Newman M E J 2018 *Networks* (Oxford: Oxford University Press)
- [10] Gilbert E 1961 Random Plane Networks *J. Soc. Indust. Appl. Math.* **9** 533–543
- [11] Penrose M 2003 *Random geometric graphs* (Oxford: Oxford University Press)
- [12] Dall J and Christensen M 2002 Random geometric graphs *Phys. Rev. E* **66** 016121
- [13] Girvan M and Newman M E J 2002 Community structure in social and biological networks *Proc. Natl. Acad. Sci. USA* **99** 7821–7826
- [14] Fontanari J F 2023 Stochastic Simulations of Casual Groups *Mathematics* **11** 2152
- [15] Fontanari J F and Santos M 2024 The dynamics of casual groups can keep free-riders at bay *Math. Biosci.* **372** 109188
- [16] Díaz-Guilera A, Gómez-Gardeñes J, Moreno Y and Nekovee M 2009 Synchronization in random geometric graphs *Int. J. Bif. Chaos* **19** 687–693
- [17] Zhang W, Lim C C, Korniss G and Szymanski B K 2014 Opinion dynamics and influencing on random geometric graphs *Sci. Rep.* **4** 5568
- [18] Reia S M, Gomes P F and Fontanari J F 2020 Comfort-driven mobility produces spatial fragmentation in Axelrod’s model *J. Stat. Mech.* **2020** 033402
- [19] Estrada E, Meloni S, Sheerin M and Moreno Y 2016 Epidemic spreading in random rectangular networks *Phys. Rev. E* **94** 052316
- [20] Gomes P F, Reia S M, Rodrigues F A and Fontanari J F 2019 Mobility helps problem-solving systems to avoid groupthink *Phys. Rev. E* **99** 032301
- [21] Stauffer D and Aharony A 1994 *Introduction To Percolation Theory* (New York: Taylor & Francis)
- [22] Clauset A, Shalizi C R and Newman M E J (2009) Power-Law Distributions in Empirical Data *SIAM Review.* **51** 661–703
- [23] Newman M E J 2005 Power laws, Pareto distributions and Zipf’s law *Contemp. Phys.* **46** 323–351

- [24] Dosey M A and Meisels M (1969) Personal space and self-protection *J. Pers. Soc. Psychol.* **11** 93–97
- [25] Okubo A 1986 Dynamical aspects of animal grouping: Swarms, schools, flocks, and herds *Adv. Biophys.* **22** 1–94